

Search for Cosmic-Ray Antideuterons

H. Fuke,^{1,*} T. Maeno,^{2,†} K. Abe,^{2,‡} S. Haino,³ Y. Makida,³ S. Matsuda,⁴ H. Matsumoto,⁴
J. W. Mitchell,⁵ A. A. Moiseev,⁵ J. Nishimura,⁴ M. Nozaki,² S. Orito,^{4,§} J. F. Ormes,^{5,¶}
M. Sasaki,⁵ E. S. Seo,⁶ Y. Shikaze,^{2,**} R. E. Streitmatter,⁵ J. Suzuki,³ K. Tanaka,³ K. Tanizaki,²
T. Yamagami,¹ A. Yamamoto,³ Y. Yamamoto,^{4,††} K. Yamato,² T. Yoshida,³ and K. Yoshimura³

¹*Institute of Space and Astronautical Science (ISAS/JAXA), Sagami-hara, Kanagawa 229-8510, Japan*

²*Kobe University, Kobe, Hyogo 657-8501, Japan*

³*High Energy Accelerator Research Organization (KEK), Tsukuba, Ibaraki 305-0801, Japan*

⁴*The University of Tokyo, Tokyo 113-0033, Japan*

⁵*NASA, Goddard Space Flight Center, Greenbelt, MD 20771*

⁶*University of Maryland, College Park, MD 20742*

(Dated: November 5, 2018)

We performed a search for cosmic-ray antideuterons using data collected during four BESS balloon flights from 1997 to 2000. No candidate was found. We derived, for the first time, an upper limit of 1.9×10^{-4} (m²s sr GeV/nucleon)⁻¹ for the differential flux of cosmic-ray antideuterons, at the 95% confidence level, between 0.17 and 1.15 GeV/nucleon at the top of the atmosphere.

PACS numbers: 98.70.Sa, 95.85.Ry, 96.40.De, 97.60.Lf

The possible presence of various species of antimatter in the cosmic radiation can provide evidence of sources and processes important for both astrophysics and elementary particle physics.

For example, discovery of a single antihelium nucleus in the cosmic radiation would offer clear evidence for a baryon symmetric cosmology. Despite extensive and ongoing searches, none has ever been found [1, 2].

Similarly, the spectral form and magnitude of the antiproton (\bar{p}) spectrum could provide evidence for a number of possible primary sources, including evaporating primordial black holes (PBHs) [3, 4] and annihilating neutralino dark matter [5, 6] as well as a baryon symmetric cosmology. However, recent results from the BESS experiment [7, 8, 9] imply that most of the \bar{p} 's in the cosmic radiation are not from primary sources, but rather are secondary products of the energetic collisions of Galactic cosmic rays with the interstellar medium. The data do suggest that below ~ 1 GeV there is an excess of \bar{p} 's above expectation from a purely secondary origin, but the situation is far from clear. Model calculations of the secondary spectrum still have ambiguities [3, 5, 10, 11, 12] and statistical errors of the currently measured low-energy \bar{p} spectrum are not small enough to provide clarity. The accuracy of both calculations and measurements needs substantial improvement.

While antideuterons (\bar{d} 's) have never been detected in the cosmic radiation, they can be produced by the same sources as \bar{p} 's and may be of both secondary or primary origin, with the latter providing evidence for sources such as PBHs and annihilating neutralino dark matter. The low energy range below ~ 1 GeV/nucleon offers a unique window in the search for cosmic-ray primary \bar{d} 's because it has a greatly reduced background from secondary \bar{d} 's [13, 14, 15], as compared with secondary \bar{p} 's. Thus, the unambiguous detection of a single

\bar{d} below ~ 1 GeV/n would strongly suggest the existence of novel primary origins. Hence, cosmic-ray \bar{d} 's have an advantage over cosmic-ray \bar{p} 's as a probe to search for primary origins.

In this paper we report on a search for \bar{d} 's carried out with four balloon flights of the BESS instrument from 1997 to 2000. Using data from these flights, we report for the first time an upper limit on the differential flux of cosmic-ray \bar{d} 's and discuss this result in the context of expectation from evaporating PBHs.

The BESS detector was designed [16, 17] and developed [18] as a high-resolution spectrometer with the large geometrical acceptance and strong particle-identification capability required for antimatter searches. A uniform magnetic field of 1 Tesla is generated by a thin superconducting solenoid. The field region is filled with tracking detectors consisting of a jet-type drift chamber (JET) and two inner drift chambers (IDCs). Tracking is performed by fitting up to 28 hit points in these drift chambers, resulting in a rigidity (R) resolution of 0.5% at 1 GV. The upper and lower time-of-flight scintillator hodoscopes (TOFs) measure the velocity (β) and the energy loss (dE/dx). The time resolution of each counter is 55 ps, which yields a $1/\beta$ resolution of 1.4%. A threshold-type Čerenkov counter with a silica-aerogel radiator ($n=1.03$ in 1997 and $n=1.02$ thereafter) can reject e^-/μ^- events, which can be backgrounds for the detection of \bar{p} 's and \bar{d} 's, by a factor of $\sim 10^3$.

Four balloon flights were carried out in northern Canada, 1997 through 2000: from Lynn Lake to Peace River where the geomagnetic cutoff rigidity ranges from 0.3 to 0.5 GV. Data for the \bar{d} search were taken for live time of 15.8, 16.8, 27.4, and 28.7 hours in 1997, 1998, 1999, and 2000 respectively, at altitudes around 36 km, corresponding to ~ 5 g/cm² in residual atmospheric depth. The data acquisition sequence was ini-

tiated by a first-level trigger, which is generated by a coincidence between hits of the top and bottom TOFs with a threshold set at 1/3 of the pulse height from minimum ionising particles. In addition to biased trigger modes [8, 18] enriching negatively charged particles, one of every 60 (30 in 2000) first-level triggered events were recorded as unbiased samples.

The concept of the off-line analysis is similar to that used for the \bar{p} selection described in Ref [8]. For events of both negative and positive curvature, same selections were applied to detect clear \bar{d} and deuteron (d) candidates. The selected d 's were used to estimate selection efficiencies for \bar{d} 's. At the first step, we selected events with a single downward-going, passing-through track which is fully contained inside the fiducial volume with restricted number of TOF hits, in order to reject interacted events as well as albedo particles. At the second step, in order to eliminate backgrounds such as large-angle scattered events by ensuring good quality of R and β measurements, we applied several cuts on tracking and timing measurement quality parameters such as: (i) the number of used hits and the reduced χ^2 of the trajectory fitting, and (ii) the consistency between the JET track, hits in the IDCs, and the TOF timing information.

In order to identify \bar{d} 's, dE/dx measurements inside the TOFs and the JET were required to be consistent with d 's as a function of R . In addition, the Čerenkov veto was applied to reduce the e^-/μ^- background contamination. Thereafter, the mass of the incident particle was reconstructed using the measured β and R . Figure 1 shows the $1/\beta$ vs. R plots of the events which survived all the above selections (for 1997 – 1999, only the negative rigidity events are shown). The \bar{d} selection region was determined by the mirror position of the d band, which was defined to have a uniform selection efficiency of 99%. In order to avoid the contamination (or misidentification) of \bar{p} 's, the region overlapped by the \bar{p} band was excluded. The exclusion band was defined so that it had a uniform selection efficiency for \bar{p} 's and the possible \bar{p} contamination from the whole data set was just one event or less in an estimation using the $1/\beta$ distributions of positively charged particles. The contamination of other negatively charged particles (mainly e^-/μ^-) was estimated to be less than 0.1 event. The possibility of the spill over of positively charged particles into the negative side is negligible in the considered rigidity region. In Fig. 1 (panel BESS00), candidates of protons (p 's) and \bar{p} 's selected by the same procedure are superimposed.

As shown in Fig. 1, clear mass bands of p 's, d 's, tritium and \bar{p} 's can be seen. However, no \bar{d} candidate exists within the expected selection region.

Since no \bar{d} candidate was found, we calculated the resultant upper limit on the \bar{d} flux [19], $\Phi_{\bar{d}}$, which is given by: $\Phi_{\bar{d}} = N_{\text{obs}} / |S\Omega \varepsilon_{\text{total}} (1 - \delta_{\text{sys}})|_{\text{min}} / T_{\text{live}} / (E_2 - E_1)$. The live time, T_{live} , was directly measured by a 1 MHz-clock pulse generator and scalers throughout the flights.

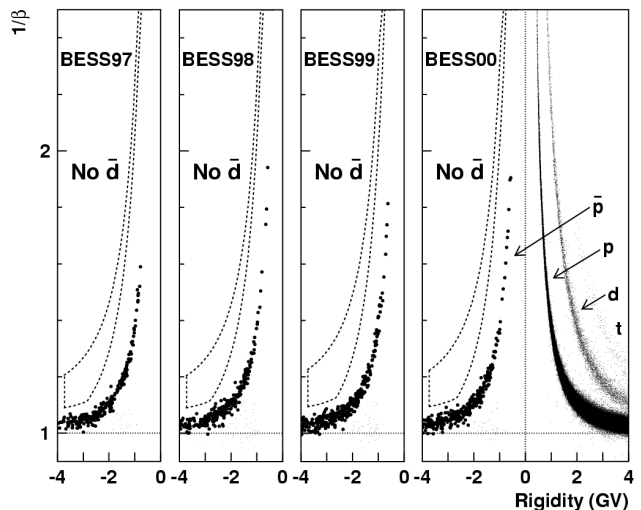


FIG. 1: The surviving single-charge events in the data of each flight. The dotted curves define the \bar{d} mass bands. The dotted vertical lines at ~ -3.7 GV corresponds to E_2 shown in Fig. 2.

As the number of the observed \bar{d} events, N_{obs} , we took 3.09 for the calculation of the 95% C.L. upper limit. We did not consider the effect of the possible background contamination ($\lesssim 1$ event), because the background estimation still has an ambiguity since it is difficult to evaluate the amount of the tail distribution strictly. E_1 and E_2 denote the energy range of the limit at the top of the atmosphere (TOA). The energy measured at the instrument was traced back to the one at the TOA by correcting the ionisation energy loss. In order to obtain the most conservative limit, the minimum value of $(S\Omega \varepsilon_{\text{total}} (1 - \delta_{\text{sys}}))$ was used, where $S\Omega$ is the geometrical acceptance, $\varepsilon_{\text{total}}$ is the total detection efficiency, and δ_{sys} is the total systematic uncertainty. The $\varepsilon_{\text{total}}$ can be written as $\varepsilon_{\text{total}} = \varepsilon_{\text{trig}} \varepsilon_1 \varepsilon_2 \varepsilon_{\text{pid}} \varepsilon_{\text{acc}} \varepsilon_{\text{air}}$. The efficiency of the first step selection including the effects of inelastic interactions in the instrument (ε_1), the survival probability in the residual atmosphere (ε_{air}), and the $S\Omega$ were calculated by the BESS Monte Carlo (MC) based on GEANT/GHEISHA. Since there are no experimental data of \bar{d} interactions in material, we incorporated the \bar{d} in the code under the following assumptions: (i) The inelastic cross sections of \bar{d} can be estimated by scaling those of \bar{p} using an empirical model of hard spheres with overlaps [20, 21], which is described as: $\sigma(A_i, A_t) \propto [A_i^{1/3} + A_t^{1/3} - 0.71 \times (A_i^{-1/3} + A_t^{-1/3})]^2$; where $\sigma(A_i, A_t)$ is the cross section of an incident particle with atomic weight A_i to a target with atomic weight A_t . (ii) When an inelastic interaction occurs, \bar{d} is always fragmented or annihilated. (iii) Other effects of energy loss, multiple scattering, bremsstrahlung and δ -rays are described as are those of other nuclei. This

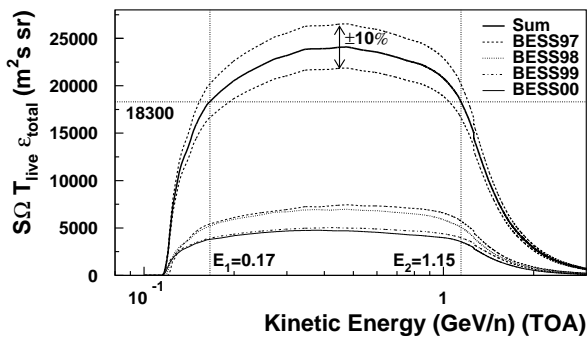


FIG. 2: Effective exposure factors of each flight data and their sum. The systematic uncertainty is shown as a $\pm 10\%$ width band. E_1 and E_2 denote the energy range of the limit.

hard sphere model is known to reproduce data on nuclear interactions for various combinations of A_i and A_t including light nuclei such as p/d [21, 22] and antinuclei including \bar{p}/\bar{d} [23, 24]. We adopted this model to estimate the $\sigma(\bar{d}, A_t)$ scaling from the $\sigma(\bar{p}, A_t)$ described in Ref. [25]. The efficiency of the the second step selection (ε_2) was estimated by using both the unbiased data and the BESS MC. The trigger efficiency ($\varepsilon_{\text{trig}}$) was obtained by using the unbiased data and a detector beam-test data [25]. The efficiency of particle identification (ε_{pid}) was estimated using the unbiased d samples of each flight under the assumption that the \bar{d} candidate should behave similarly to d except for deflection in the symmetrical configuration of BESS. Typical values at 0.5 GeV/n are: $\varepsilon_{\text{trig}} \sim 90\%$, $\varepsilon_1 \sim 60\%$, $\varepsilon_2 \sim 70\%$, $\varepsilon_{\text{pid}} \sim 98\%$, $\varepsilon_{\text{air}} \sim 85\%$, and $S\Omega \sim 0.25 \text{ m}^2\text{sr}$. The probability of events without any hits or tracks by another accidental incident particle, ε_{acc} , was derived to be $\sim 94\%$ by samples taken by the random trigger which was issued at once a second throughout the flights.

Figure 2 shows the calculated effective exposure factor. The decrease of the factor at the low-energy side is mainly caused by the decrease of the geometrical acceptance, the decrease of mean free path through the detector, and the increase of large-angle scattering. The major reason for the decrease at the high-energy side is the decrease of ε_{pid} due to the overlap of $1/\beta$ distributions between \bar{d} 's and \bar{p} 's. The combined systematic uncertainty, which was estimated to be $\delta_{\text{sys}} \sim 10\%$ with less energy dependence, is also shown in the figure. Dominant systematic uncertainties were the uncertainties in the evaluation of ε_1 , ε_2 and ε_{air} , all of which were discussed using the MC simulation. The energy range of $E_1 - E_2$ was chosen to be 0.17 – 1.15 GeV/n, where the exposure factor is highest and has relatively little energy dependence.

The resultant upper limit $\Phi_{\bar{d}}$ for 1997, 1998, 1999, 2000, and the integrated flight data were calculated to be 9.8, 8.9, 6.9, 6.2, and $1.9 \times 10^{-4} \text{ (m}^2\text{s sr}^2\text{GeV/n)}^{-1}$ respectively (Fig. 3). These are the most conservative

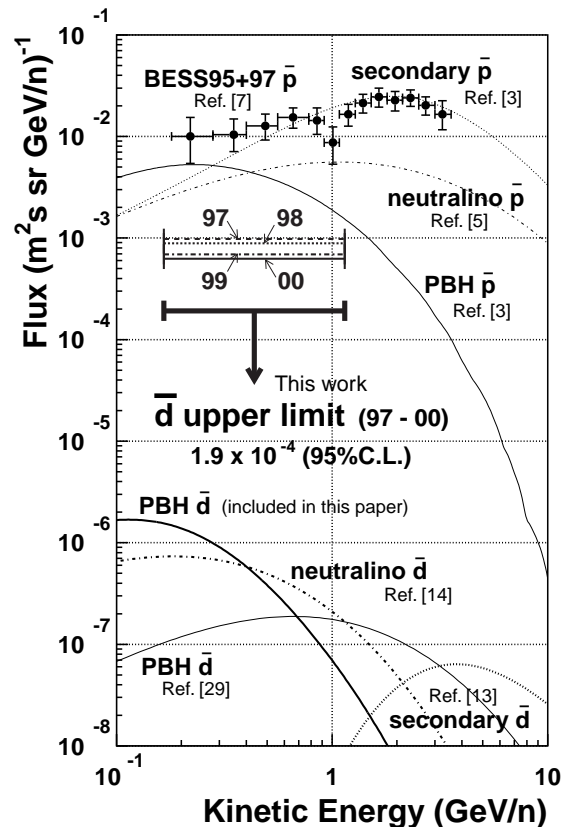


FIG. 3: Obtained upper limit on the \bar{d} flux in comparison with the PBH- \bar{d} spectrum calculated in this paper. A \bar{p} spectrum measured by BESS and some theoretically predicted spectra of \bar{p} and \bar{d} are shown for reference.

limits with no assumptions on the \bar{d} spectrum shape. If we assume a uniform \bar{d} energy spectrum and use a mean inverse exposure factor, the summed upper limit was evaluated to be 1.6×10^{-4} in the same energy range, and 1.4×10^{-4} in the range 0.13 – 1.44 GeV/n where the upper limit is minimized under this assumption. Since our detection efficiency of \bar{d} is less dependent on the energy, the upper limit is less dependent on the assumption of the \bar{d} spectrum shape. In the following discussions, we use the most conservative one (1.9×10^{-4}).

As described in Ref. [3], only PBHs that are close to explosion and exist within a few kpc of the solar system can contribute to the observed flux. Therefore, the \bar{d} upper limit leads directly to the upper limit on the explosion rate of local PBHs, \mathcal{R}_{PBH} . In order to obtain \mathcal{R}_{PBH} from the \bar{d} upper limit, we have calculated an expected PBH- \bar{d} spectrum through the following steps: (i) the emission rate of particles from PBHs, (ii) the fragmentation rate to form \bar{d} 's, (iii) the source spectrum, (iv) the propagation process, and (v) the effect of the solar modulation. The calculations except for (ii) were based on the calculation of PBH- \bar{p} spectrum de-

scribed in Ref. [3]. The step (ii) was performed by using the frequently-used “coalescence model” (e.g. Ref. [26]). According to this model, the production probability of \bar{d} 's in momentum space, $d^3n_{\bar{d}}/dp^3$, can be expressed as the product of those of \bar{p} 's and antineutrons: $\gamma \frac{d^3n_{\bar{d}}}{dp^3} = \frac{4}{3}\pi p_0^3 \left(\gamma \frac{d^3n_{\bar{p}}}{dp^3}\right) \left(\gamma \frac{d^3n_{\bar{n}}}{dp^3}\right) \approx \frac{4}{3}\pi p_0^3 \left(\gamma \frac{d^3n_{\bar{p}}}{dp^3}\right)^2$, where p_0 is the “coalescence momentum” which must be determined from experiments. We assumed $p_0 = 130$ MeV/c from the data of \bar{d} production in e^+/e^- annihilation [27]. The solar modulation in step (v) was estimated by using the numerical solution of the spherically symmetric model proposed by Fisk [28]. The solar modulation parameter, ϕ , was determined to fit the p spectrum measured in the same BESS flights as: 500, 610, 648, and 1334 MV in 1997, 1998, 1999, and 2000 respectively [8, 9]. The calculated PBH- \bar{d} flux for 1997 on the assumption of $\mathcal{R}_{\text{PBH}} = 2.2 \times 10^{-3} \text{ pc}^{-3}\text{yr}^{-1}$ is shown in Fig. 3. The difference between our PBH- \bar{d} flux and the one in Ref. [29] mainly comes from the different assumptions on the propagation model, similar to the case of the difference in the PBH- \bar{p} spectrum between Ref. [3] and Ref. [4] that is described in Ref. [4].

Here, we place the upper limit on the \mathcal{R}_{PBH} to be $1.8 \times 10^0 \text{ pc}^{-3}\text{yr}^{-1}$, which is five orders of magnitude more stringent than the sensitivity for 50-TeV γ -ray bursts [30]. The limit on \mathcal{R}_{PBH} leads to an upper limit on the density parameter of PBHs in the Universe, Ω_{PBH} , to be 1.2×10^{-6} . The initial mass spectrum of PBHs was assumed to have a $-\frac{5}{2}$ power-law form, and the PBH spatial distribution was assumed to be proportional to the mass density distribution of dark matter within the galactic halo [3].

As a conclusion, we have searched for cosmic-ray \bar{d} 's with the BESS flight data obtained between 1997 and 2000. No \bar{d} candidate has been detected. We placed, for the first time, an upper limit of $1.9 \times 10^{-4} (\text{m}^2\text{s sr GeV/n})^{-1}$ (95% C.L.) on the differential flux of cosmic-ray \bar{d} 's in an energy range of 0.17 – 1.15 GeV/n at the top of the atmosphere. In consequence, we derived an upper limit of $1.8 \times 10^0 \text{ pc}^{-3}\text{yr}^{-1}$ (95% C.L.) on the explosion rate of local PBHs and an upper limit of 1.2×10^{-6} (95% C.L.) on the density parameter of PBHs.

These upper limits regarding PBHs are two orders of magnitude looser than those derived from the \bar{p} flux [3]. However, further sensitive searches could push down the limits from \bar{d} 's below the ones from \bar{p} 's, because the low-energy range has a greatly reduced background from secondary \bar{d} 's. Astrophysical consequences of our \bar{d} search will motivate further sensitive searches for \bar{d} 's as well as further advances in the physics of primary origins, in connection with cosmology and elementary particle physics.

We would like to thank NASA, NSBF, KEK, ISAS and ICEPP for their continuous support. This experiment

was supported by a Grants-in-Aid, KAKENHI (9304033, 11440085, and 11694104), from MEXT and by Heiwa Nakajima Foundation in Japan; and by NASA SR&T research grants in the USA.

-
- * E-mail address: fuke@balloon.isas.jaxa.jp
 - † Present address: BNL, Upton, NY 11973
 - ‡ Present address: ICRR, Kashiwa, Chiba 227-8582, Japan
 - § Deceased
 - ¶ Present address: Univ. of Denver, Denver, CO 80208
 - ** Present address: JAERI, Tokai, Ibaraki 391-1195, Japan
 - †† Present address: KEK, Tsukuba, Ibaraki 305-0801, Japan
 - [1] M. Sasaki *et al.*, Nuc. Phys. B (Proc. Suppl.) **113**, 202 (2002).
 - [2] J. Alcaraz *et al.*, Phys. Lett. B **461**, 387 (1999).
 - [3] K. Maki, T. Mitsui and S. Orito, Phys. Rev. Lett. **76**, 3474 (1996); T. Mitsui, K. Maki and S. Orito, Phys. Lett. B **389**, 169 (1996).
 - [4] A. Barrau *et al.*, Astron. Astrophys. **388**, 676 (2002).
 - [5] L. Bergström, J. Edsjö and P. Ullio, Astrophys. J. **526**, 215 (1999).
 - [6] F. Donato *et al.*, Phys. Rev. D **69**, 063501 (2004).
 - [7] S. Orito *et al.*, Phys. Rev. Lett. **84**, 1078 (2000).
 - [8] T. Maeno *et al.*, Astropart. Phys. **16**, 121 (2001).
 - [9] Y. Asaoka *et al.*, Phys. Rev. Lett. **88**, 051101 (2002).
 - [10] J. W. Bieber *et al.*, Phys. Rev. Lett. **83**, 674 (1999).
 - [11] I. V. Moskalenko *et al.*, Astrophys. J. **586**, 1050 (2003).
 - [12] F. Donato *et al.*, Astrophys. J. **563**, 172 (2001).
 - [13] P. Chardonnet, J. Orloff and P. Salati, Phys. Lett. B **409**, 313 (1997).
 - [14] F. Donato, N. Fornengo and P. Salati, Phys. Rev. D **62**, 043003 (2000).
 - [15] K. Mori *et al.*, Astrophys. J. **566**, 604 (2002).
 - [16] S. Orito, KEK Report 87-19, *Proc. of the ASTROMAG Workshop* (1987) p.111.
 - [17] A. Yamamoto *et al.*, IEEE Trans. Magn. **24**, 1421 (1988).
 - [18] Y. Ajima *et al.*, Nucl. Instrum. Methods A **443**, 71 (2000); Y. Asaoka *et al.*, Nucl. Instrum. Methods A **416**, 236 (1998); Y. Shikaze *et al.*, Nucl. Instrum. Methods A **455**, 596 (2000); Y. Makida *et al.*, IEEE Trans. Appl. Supercon. **5**, 658 (1995).
 - [19] The upper limit on the absolute \bar{d} flux is the best indicator of the sensitivity of the search for the primary sources (rather than the d/\bar{d} flux ratio for example).
 - [20] H. L. Bradt and B. Peters, Phys. Rev. **77**, 54 (1950).
 - [21] N. S. Grigalashvili *et al.*, Sov. J. Nucl. Phys. **48**, 301 (1988).
 - [22] E. O. Abdrhmanov *et al.*, Z. Physik C **5**, 1 (1980).
 - [23] T. F. Hoang *et al.*, Z. Physik C **29**, 611 (1985).
 - [24] C. Adler *et al.*, Phys. Rev. Lett. **87**, 262301 (2001).
 - [25] Y. Asaoka *et al.*, Nucl. Instrum. Methods A **489**, 170 (2002).
 - [26] J. L. Nagle *et al.*, Phys. Rev. C **53**, 367 (1996).
 - [27] H. Albrecht *et al.*, Phys. Lett. B **236**, 102 (1990).
 - [28] L. A. Fisk, J. Geophys. Res. **76**, 221 (1971).
 - [29] A. Barrau *et al.*, Astron. Astrophys. **398**, 403 (2003).
 - [30] M. Amenomori *et al.*, *Proc. 24th ICRC*, 112 (1995).